

## Frustrated Lewis Pairs in Ionic Liquids and Molecular Solvents - Neutron Scattering and NMR Study of Encounter Complexes

Lucy C. Brown, James M. Hogg, Mark Gilmore, Leila Moura, Silvia Imberti, Sabrina Gärtner, H. Q. Nimal Gunaratne, Ruairi J. O'Donnell, Nancy Artioli, John D. Holbrey\* and Małgorzata Swadźba-Kwaśny\*

### SUPPLEMENTARY INFORMATION

#### Experimental

All manipulations were performed in a nitrogen-filled MBraun glovebox with a high capacity recirculator (< 1 ppm of O<sub>2</sub> and H<sub>2</sub>O). Tris(*tert*-butyl)phosphine was purchased from Sigma-Aldrich and used as received. B(C<sub>6</sub>F<sub>5</sub>)<sub>3</sub> was obtained from Fluorochem and purified by vacuum sublimation. [C<sub>10</sub>mim][NTf<sub>2</sub>] was dried by thionyl chloride and dried *in vacuo* at 65 °C, and moisture content by Karl-Fisher was under the detection limit. Benzene-*d*<sub>6</sub> and benzene were dried over sieves and distilled. NMR spectra were recorded on a Bruker Avance DPX 400 MHz spectrometer.

#### NMR spectra for isolated components

**B(C<sub>6</sub>F<sub>5</sub>)<sub>3</sub> in benzene-*d*<sub>6</sub>** - In a nitrogen filled MBraun glovebox B(C<sub>6</sub>F<sub>5</sub>)<sub>3</sub> benzene-*d*<sub>6</sub> at a concentration of 160 mmol was transferred into a flame dried Norell IPV valved NMR sample tube for intermediate pressure.

**Tris(*tert*-butyl)phosphine in benzene-*d*<sub>6</sub>** - In a nitrogen filled MBraun glovebox tris(*tert*-butyl)phosphine in benzene-*d*<sub>6</sub> at a concentration of 160 mmol was transferred into a flame dried Norell IPV valved NMR sample tube for intermediate pressure.

**B(C<sub>6</sub>F<sub>5</sub>)<sub>3</sub> in [C<sub>10</sub>mim][NTf<sub>2</sub>]** - In a nitrogen filled MBraun glovebox a mixture of B(C<sub>6</sub>F<sub>5</sub>)<sub>3</sub> and tris(*tert*-butyl)phosphine in [C<sub>10</sub>mim][NTf<sub>2</sub>] at a concentration of 100 mmol was transferred into a flame dried Norell IPV valved NMR sample tube for intermediate pressure with a DMSO-*d*<sub>6</sub> filled, sealed capillary as an external lock.

**Tris(*tert*-butyl)phosphine in [C<sub>10</sub>mim][NTf<sub>2</sub>]** - In a nitrogen filled MBraun glovebox a mixture of B(C<sub>6</sub>F<sub>5</sub>)<sub>3</sub> and tris(*tert*-butyl)phosphine in [C<sub>10</sub>mim][NTf<sub>2</sub>] at a concentration of 100 mmol was transferred into a flame dried Norell IPV valved NMR sample tube for intermediate pressure with a DMSO-*d*<sub>6</sub> filled, sealed capillary as an external lock.

#### NMR spectra for stoichiometric mixtures

**B(C<sub>6</sub>F<sub>5</sub>)<sub>3</sub> and tris(*tert*-butyl)phosphine in benzene-*d*<sub>6</sub>** - In a nitrogen filled MBraun glovebox a mixture of B(C<sub>6</sub>F<sub>5</sub>)<sub>3</sub> and tris(*tert*-butyl)phosphine in benzene-*d*<sub>6</sub> at a concentration of 160 mmol was transferred into a flame dried Norell IPV valved NMR sample tube for intermediate pressure.

Comparison of the <sup>19</sup>F and <sup>31</sup>P NMR spectra of the concentrated FLP solution in benzene-*d*<sub>6</sub> (160 mmol) with the <sup>19</sup>F NMR spectrum of BCF and <sup>31</sup>P NMR spectrum of P(*t*Bu)<sub>3</sub> in benzene-*d*<sub>6</sub> (Fig. 3) show no indication of interaction between the FLP components, consistent with the literature.<sup>1,2</sup>

However we observe an upfield shift in the  $^{19}\text{F}$  NMR spectrum, from EPSR modelling we have observed aggregation of  $\text{B}(\text{C}_6\text{F}_5)_3$  molecules in the FLP mixture which accounts for this shift.

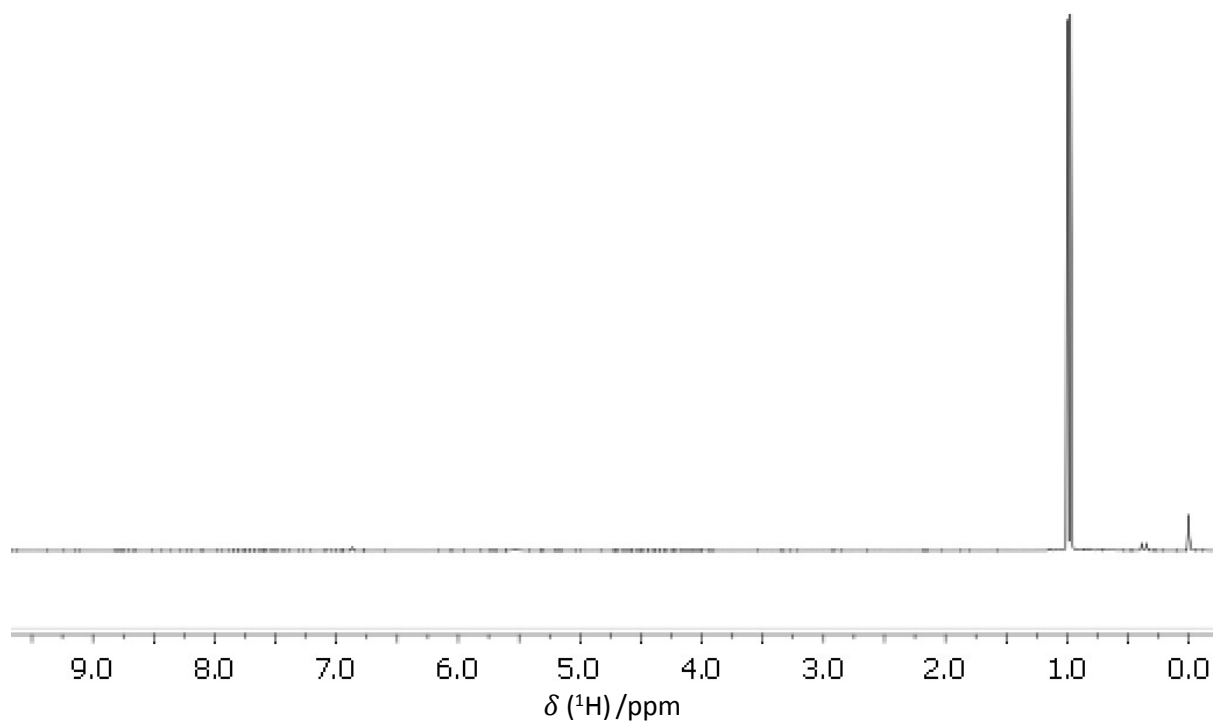


**Fig. 1-SI**  $^1\text{H}$  NMR Spectrum of  $\text{B}(\text{C}_6\text{F}_5)_3$  and tris(*tert*-butyl)phosphine in benzene- $\text{d}_6$  at a concentration of 160 mmol at ambient temperature. Major peak is phosphine protons and peak at 0 is TMS.

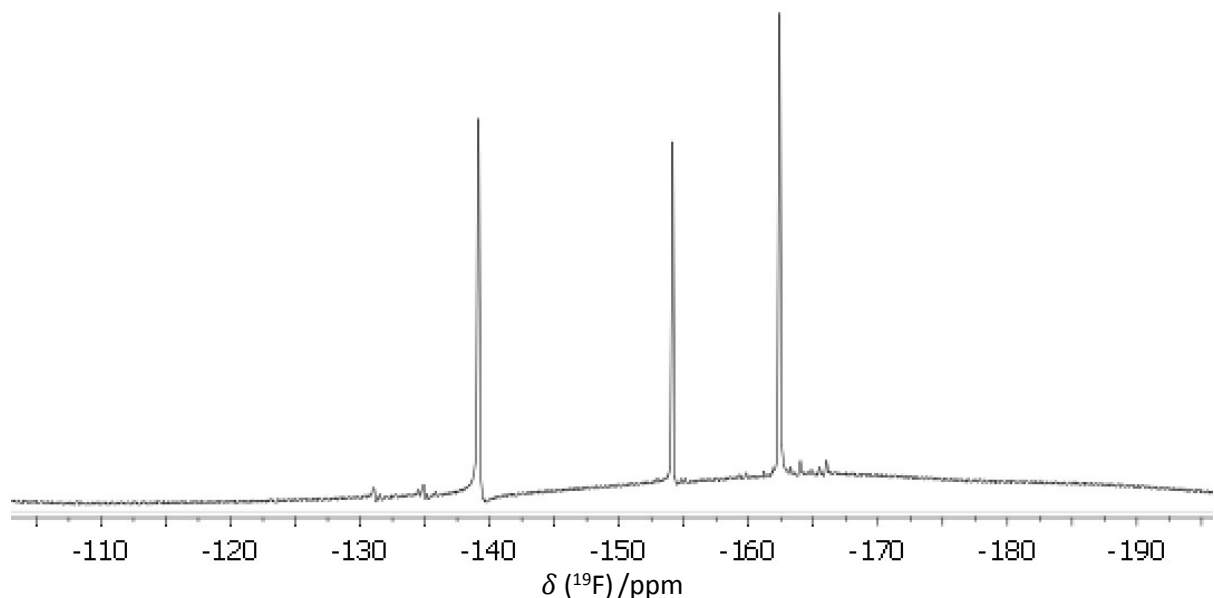


**Fig. 2-SI**  $^{19}\text{F}$  NMR Spectrum of  $\text{B}(\text{C}_6\text{F}_5)_3$  and tris(*tert*-butyl)phosphine in benzene- $\text{d}_6$  at a concentration of 160 mmol at ambient temperature.

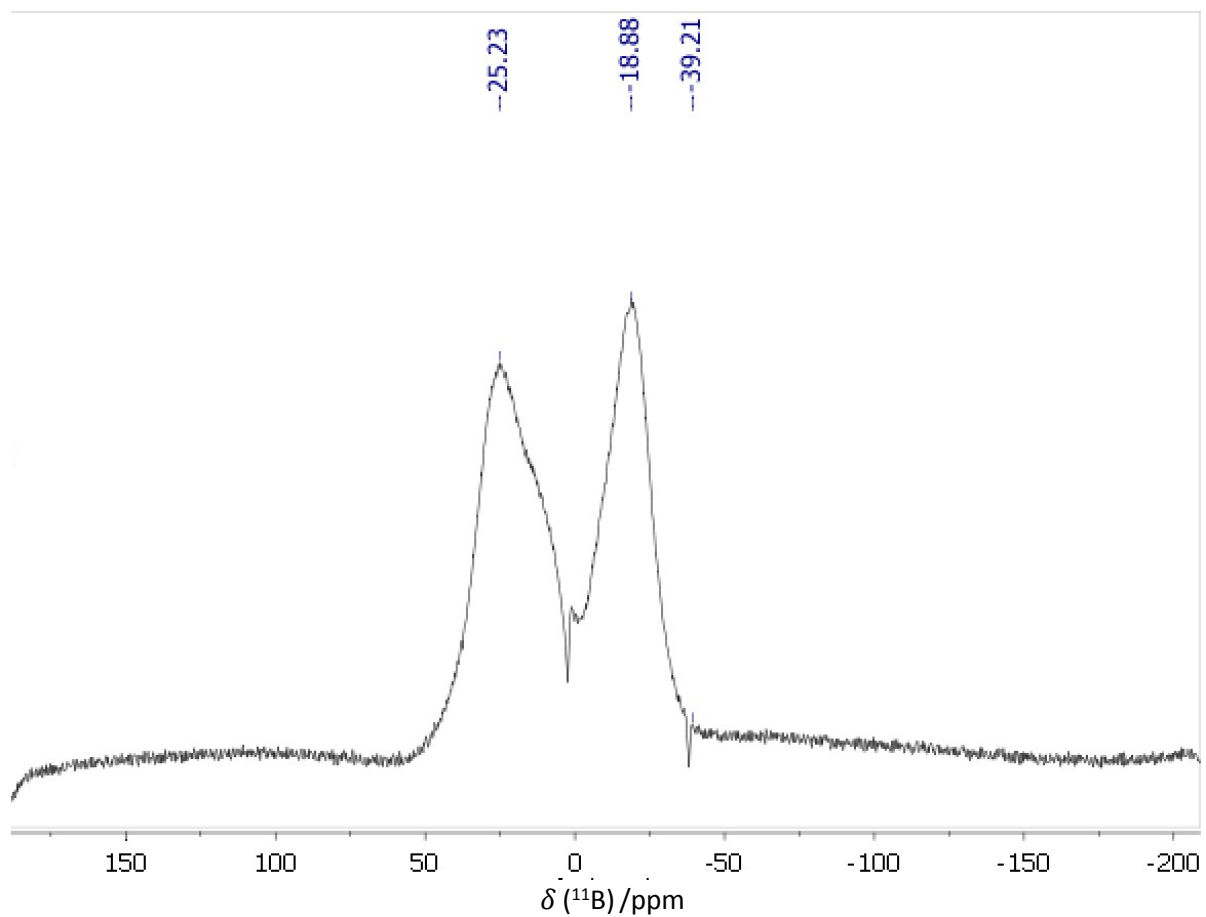


**Fig. 3-SI**  $^{11}\text{B}$  NMR Spectrum of  $\text{B}(\text{C}_6\text{F}_5)_3$  and tris(*tert*-butyl)phosphine in benzene- $\text{d}_6$  at a concentration of 160 mmol at ambient temperature showing the major peaks for the borosilicate NMR (-18 ppm) and  $\text{B}(\text{C}_6\text{F}_5)_3$  (25 ppm).

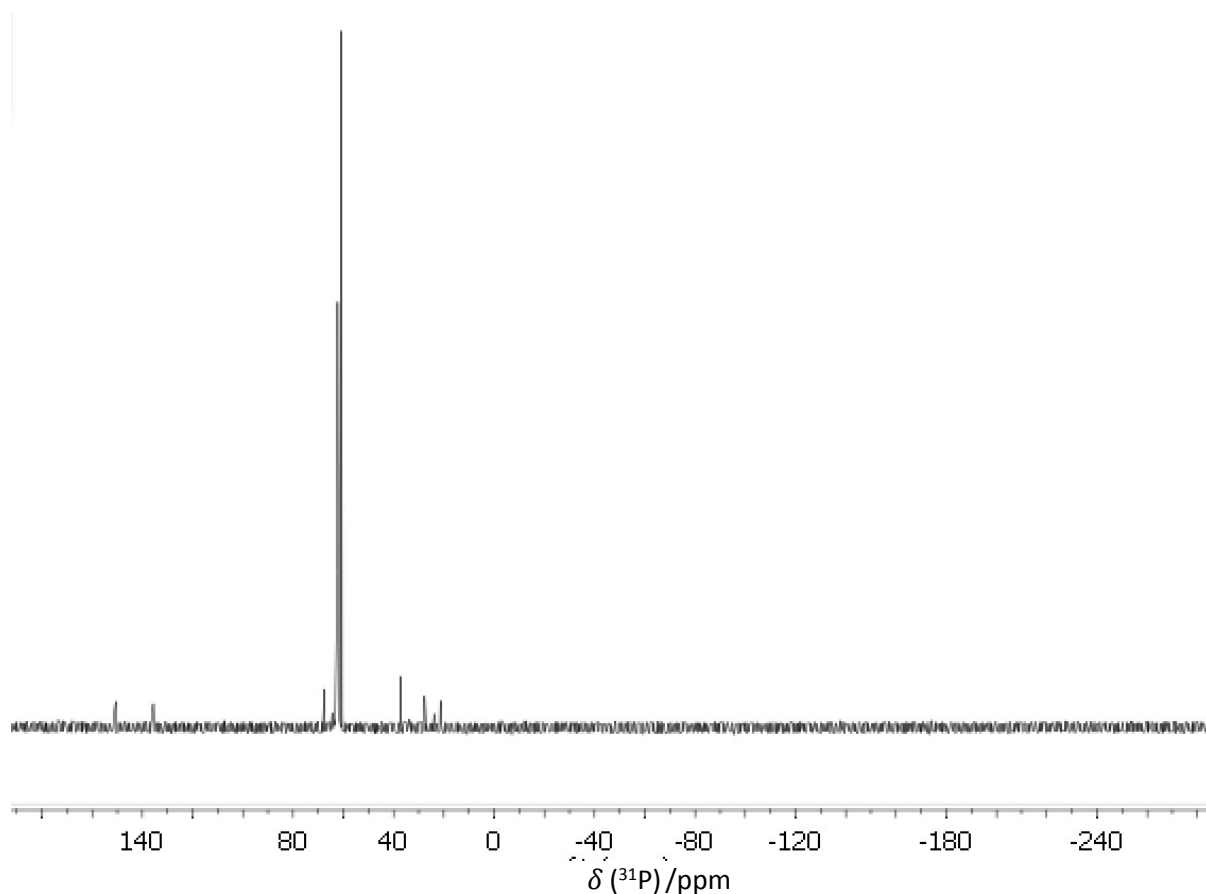


**Fig. 4-SI**  $^{31}\text{P}$  NMR Spectrum of  $\text{B}(\text{C}_6\text{F}_5)_3$  and tris(*tert*-butyl)phosphine in benzene- $d_6$  at a concentration of 160 mmol at RT

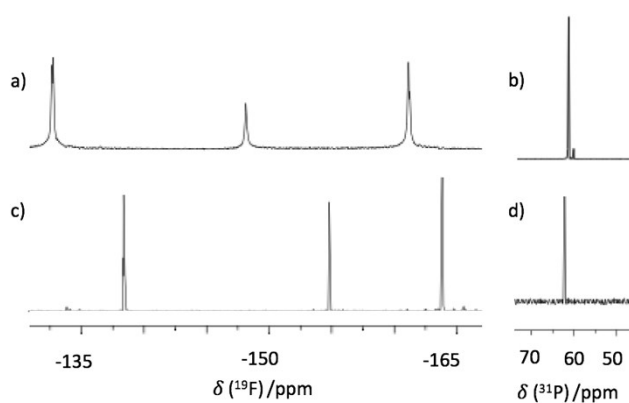


**Fig. 5 SI** NMR spectroscopy of FLP components in benzene- $d_6$ : a)  $^{19}\text{F}$  NMR spectrum of BCF, b)  $^{31}\text{P}$  NMR spectrum of  $\text{P}(\text{tBu})_3$ , c)  $^{19}\text{F}$  NMR spectrum of  $\text{P}(\text{tBu})_3/\text{BCF}$  and d)  $^{31}\text{P}$  NMR spectrum of  $\text{P}(\text{tBu})_3/\text{BCF}$ .

**$\text{B}(\text{C}_6\text{F}_5)_3$  and tris(*tert*-butyl)phosphine in  $[\text{C}_{10}\text{mim}][\text{NTf}_2]$**  - In a nitrogen filled MBraun glovebox a mixture of  $\text{B}(\text{C}_6\text{F}_5)_3$  and tris(*tert*-butyl)phosphine in  $[\text{C}_{10}\text{mim}][\text{NTf}_2]$  at a concentration of 100 mmol was transferred into a flame dried Norell IPV valved NMR sample tube for intermediate pressure with a  $\text{DMSO}-d_6$  filled, sealed capillary as an external lock.

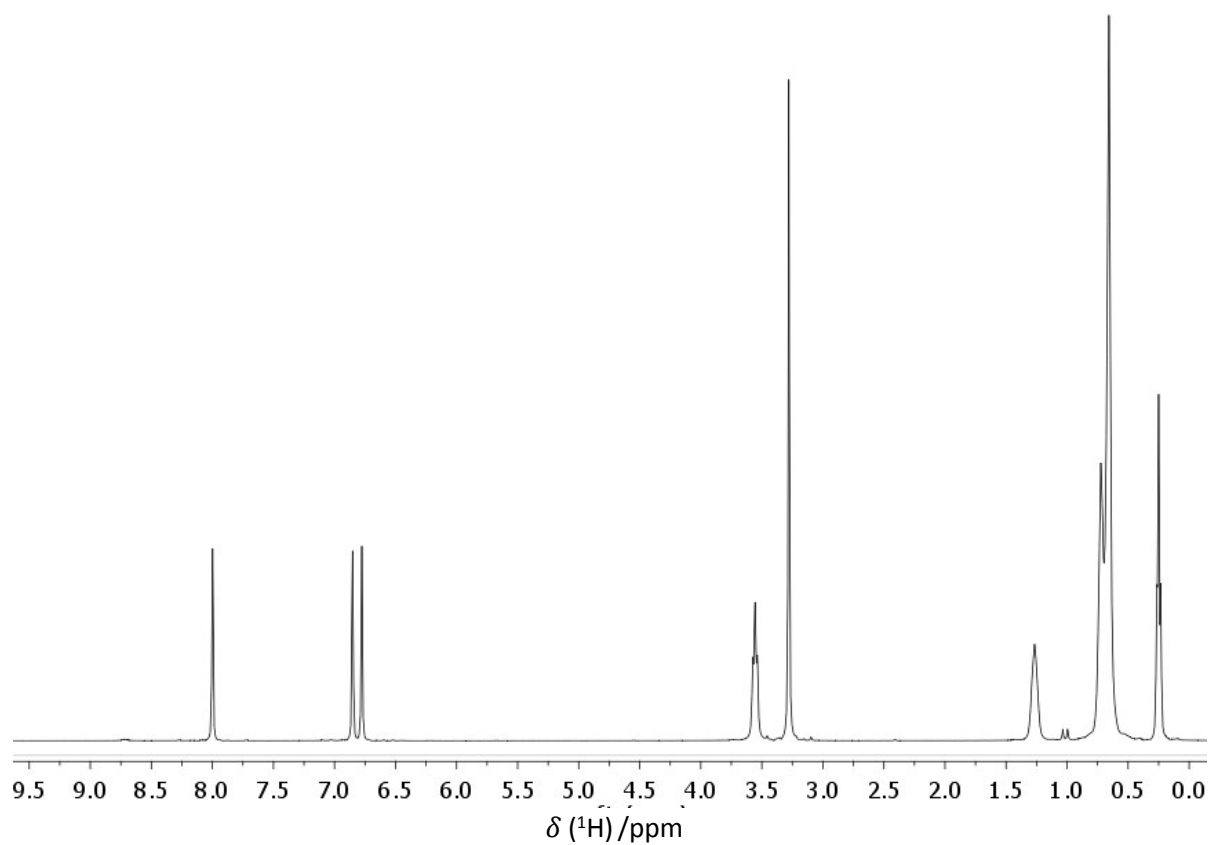


**Fig. 6-SI**  $^1\text{H}$  NMR Spectrum of  $\text{B}(\text{C}_6\text{F}_5)_3$  and  $\text{tris}(\text{tert-butyl})\text{phosphine}$  in  $[\text{C}_{10}\text{mim}][\text{NTf}_2]$  at a concentration of 160 mmol at ambient temperature with a  $\text{DMSO-d}_6$  capillary.

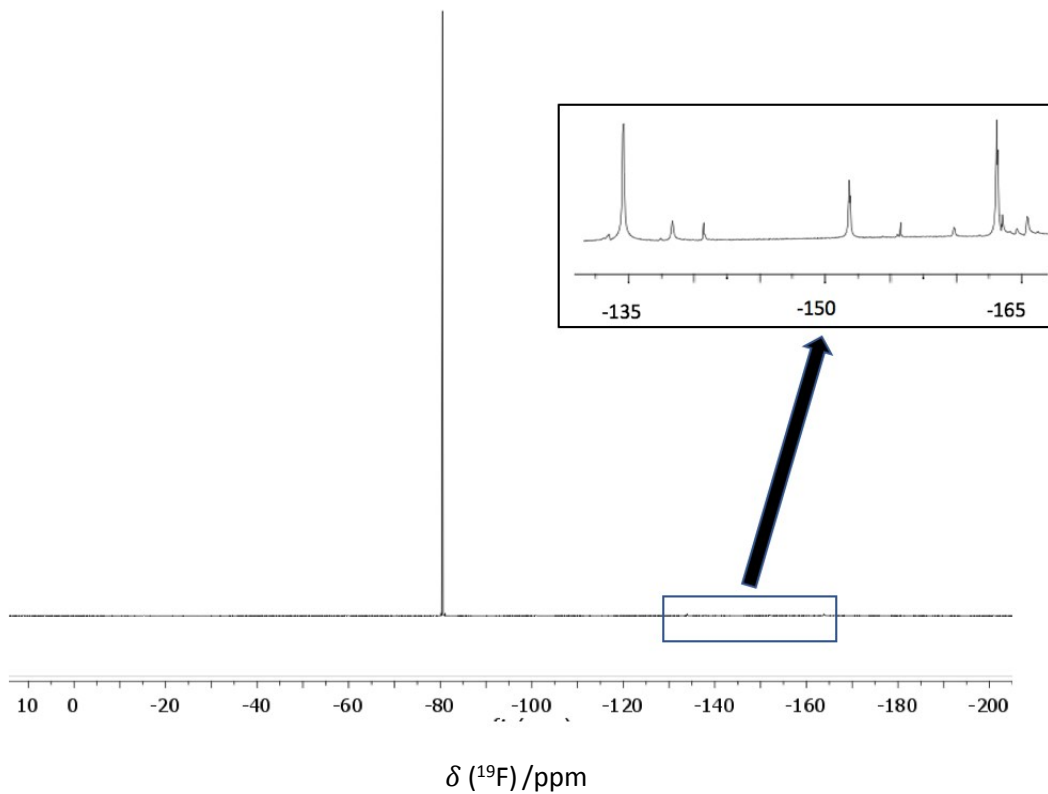


**Fig. 7-SI**  $^{19}\text{F}$  NMR Spectrum of  $\text{B}(\text{C}_6\text{F}_5)_3$  and tris(*tert*-butyl)phosphine in  $[\text{C}_{10}\text{mim}][\text{NTf}_2]$  at a concentration of 160 mmol at ambient temperature with a  $\text{DMSO-d}_6$  capillary

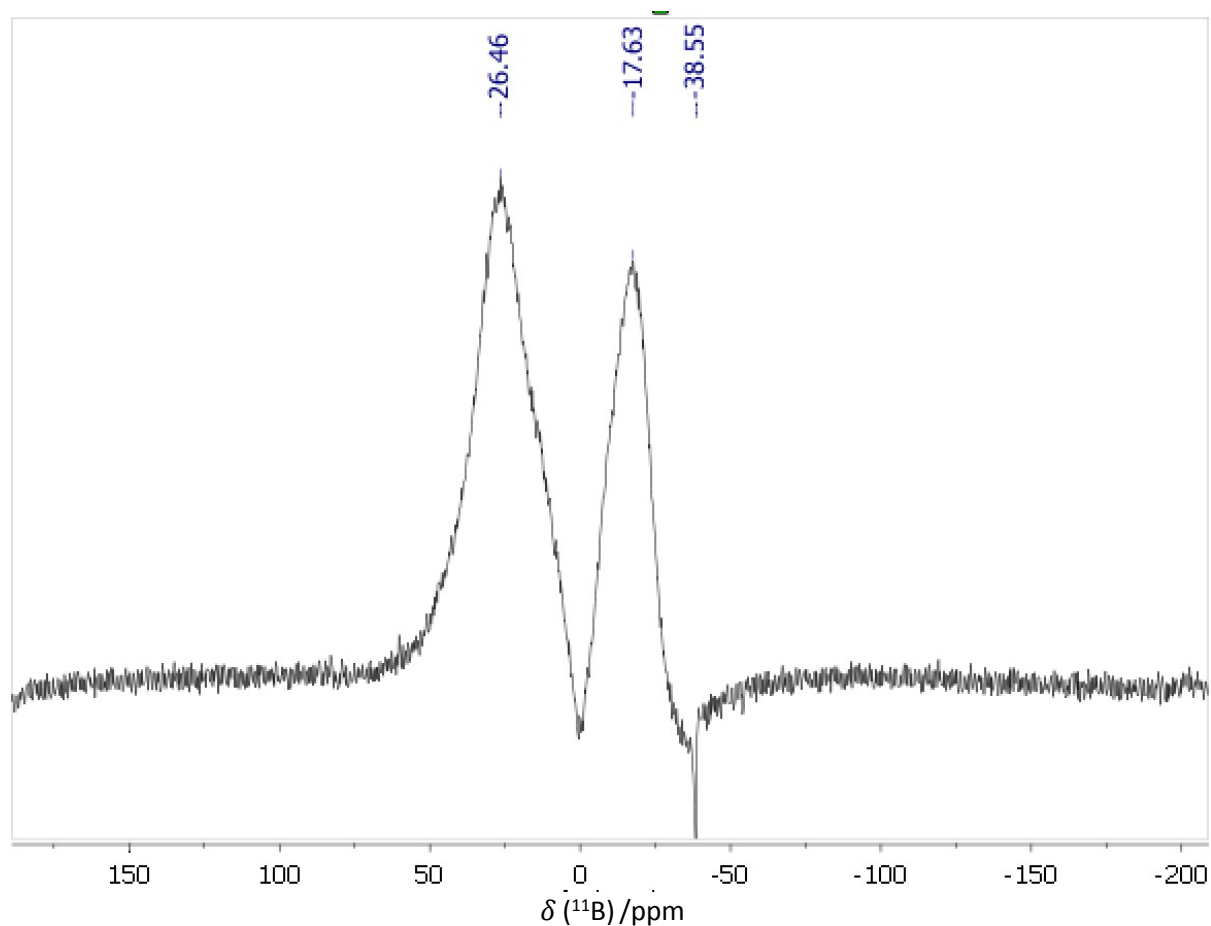


**Fig. 8-SI**  $^{11}\text{B}$  NMR Spectrum of  $\text{B}(\text{C}_6\text{F}_5)_3$  and tris(tert-butyl)phosphine in  $[\text{C}_{10}\text{mim}][\text{NTf}_2]$  at a concentration of 160 mmol at ambient temperature with a  $\text{DMSO-d}_6$  capillary showing major peaks from the borosilicate NMR tube (-17.63 ppm) and  $\text{B}(\text{C}_6\text{F}_5)_3$  (26.46 ppm).

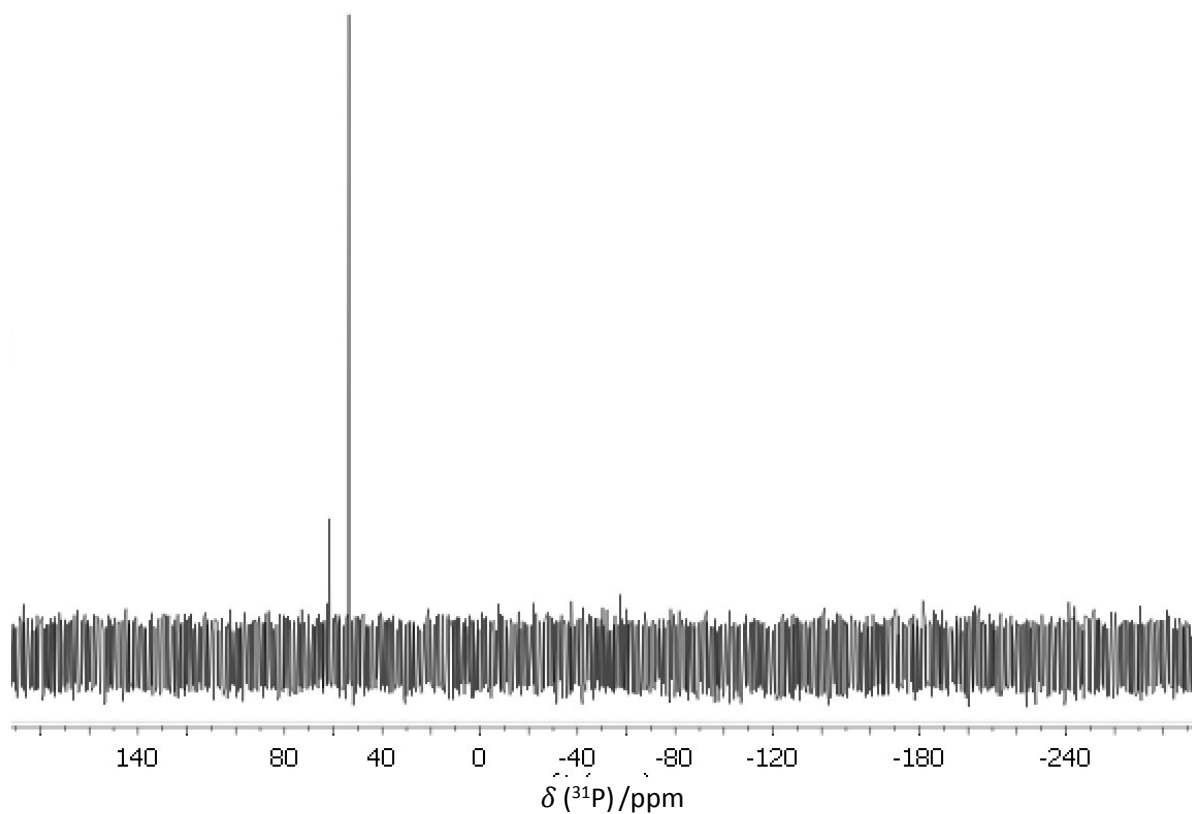


**Fig. 9-SI**  $^{31}\text{P}$  NMR Spectrum of  $\text{B}(\text{C}_6\text{F}_5)_3$  and tris(tert-butyl)phosphine in  $[\text{C}_{10}\text{mim}][\text{NTf}_2]$  at a concentration of 160 mmol at ambient temperature with a  $\text{DMSO-d}_6$  capillary.

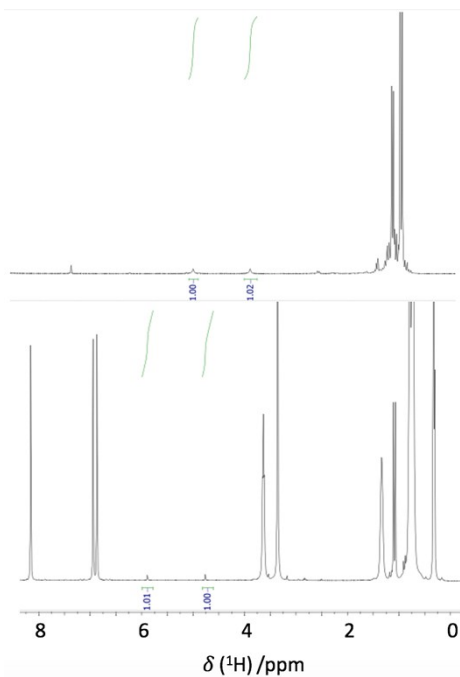


**Fig. 10 -SI.** The  $^1\text{H}$  NMR spectra of FLP with  $\text{H}_2$  in (top) benzene and (bottom)  $[\text{C}_{10}\text{mim}][\text{NTf}_2]$  showing the presence of  $\text{H}_2$ .



## Neutron scattering data from P(<sup>t</sup>Bu)<sub>3</sub> and B(C<sub>6</sub>F<sub>5</sub>)<sub>3</sub> in benzene

Neutron scattering data were collected at the ISIS pulsed neutron and muon source at the Rutherford Appleton Laboratory, UK, using the SANDALS spectrometer. Three isotopic contrast solutions were prepared at a 1:1:70 molar ratio of P(<sup>t</sup>Bu)<sub>3</sub> and B(C<sub>6</sub>F<sub>5</sub>)<sub>3</sub> in benzene using benzene-*h*<sub>6</sub>, benzene-*d*<sub>6</sub> and a 1:1 mixture of hydrogenous and deuterated benzene in an inert argon filled glovebox. Samples were loaded and sealed under argon in “null scattering” Ti<sub>0.68</sub>Zr<sub>0.32</sub> flat plate cells with internal geometries of 1×35×35 mm, with a wall thickness of 1 mm. During measurements, the cell was maintained at a temperature of 303 K using a recirculating heater (Julabo FP50). Measurements were made on each of the empty sample holders, the empty spectrometer, and a 3.1 mm thick vanadium standard sample for the purposes of instrument calibration and data normalisation.

Data from the three samples was corrected for instrument and background, and normalised using GUDRUN<sup>3</sup> to produce a differential scattering cross section for each experimental sample. The sample densities were estimated at 0.99 g cm<sup>-3</sup> (hydrogenous) and 1.06 g cm<sup>-3</sup> (deuterated) based on the actual isotopic compositions and measured scattering levels. Data was analysed using the Empirical Potential Structure Refinement (EPSR) program<sup>4</sup> to build and iteratively refine a three dimensional model of the liquid structure that is self-consistent with the experimental total structure factors, *F*(*Q*) for the three isotopically distinct samples.

The EPSR refinements were performed using 700 benzene solvent molecules and 10 molecules each of P(<sup>t</sup>Bu)<sub>3</sub> and B(C<sub>6</sub>F<sub>5</sub>)<sub>3</sub> in a cubic simulation box of dimension 47.8 Å. Models were refined against the experimental data over the full data range (*Q* = 0.1–50 Å<sup>-1</sup>). Within the EPSR simulation, initial potentials and interatomic distance constraints used to define the basic molecular geometries were obtained from MOPAC with the AM1 model. Atom types in each system were defined based on their unique positions in the molecular skeletons, as shown in **Fig. 11-SI**, and full rotational flexibility was enabled around the P and B atoms of the Lewis base and acid molecules. The full parameters of the reference potential used are given in **Table 1-SI** and the interatomic distance and angular constraints used to define the basic molecular geometries are summarised in **Table 2-SI**. Simulations were allowed to equilibrate for at least 2500 cycles before applying the empirical potential, then were equilibrated over *ca.* 10 000 cycles before accumulating and averaging data over up to 100,000 iterations. Multiple simulations were performed, starting from new randomised molecular configurations in each case.

A reasonable self-consistent model was generated for the FLP solutions in EPSR. A comparison of the experimental and EPSR generated *S*(*Q*) data from one of the refinement runs is shown in **Fig. 12-SI**. Overall, the refinement accurately reproduced the experimental data for short length inter- and intra-molecular correlations, however a relatively poor fit to the data is observed in the low *Q* region (<0.5 Å<sup>-1</sup>) where correction of the raw data for inelastic scattering from hydrogen atoms is most problematic. Indeed, correction for this scattering contribution in GUDRUN was extremely sensitive to variation in correction parameters (number of iterations for correction) leading to a poor level of confidence in the reliability of the scattering levels in this region. In order to address this, additional experimental data sets using H/D isotopic contrast on the tri-tert-butylphosphene could improve sensitivity, although it is noted that deuterated tris(tert-butyl)phosphine (PC<sub>12</sub>D<sub>27</sub>) is not a previously reported compound according to CAS.

Multiple EPSR simulations were performed, starting from unique initial configurations, in order to establish the consistency in the EPSR model to the data sets, and in order to ensure reasonable statistics from the refinement, data was accumulated over 100,000 iterations and the P⋯B correlation was extracted. This long simulation time was necessary because the number density of B and P sites in the EPSR model is very small, limited by the effective scale of simulations and the relatively low concentration of FLP in solution. A consequence of this potential variability in the experimental scattering from the data sets in the low *Q* region, corresponding to longer correlation

distances in the samples, is that models for the data generated in EPSR were not completely stable, and multiple simulations gave rise to similar, but different trajectories. This can be seen in the P...B correlations shown in **Fig. 3** (main manuscript) from two independent models. The low number of specific P and B sites in the simulation models (0.2% of the atoms in the simulation box are P or B, although 7% of all the atoms in the system are part of either the Lewis acid or base components) also result in very slow accumulation of data points for the P...B correlation and so relatively poor statistical averaging of outlying correlations. Consequently, specific features at short correlation lengths (<6 Å) observable in some simulations cannot be regarded as clear evidence for interactions, whereas the common peak between 7-9 Å which appears in all the refinements does appear to show some definitive evidence for an association at around the solvent-separated pair distance.

Radial distribution functions between P(<sup>t</sup>Bu)<sub>3</sub> and B(C<sub>6</sub>F<sub>5</sub>)<sub>3</sub> were extracted directly from the B...P site-site partial radial distribution function calculated within EPSR, and for P(<sup>t</sup>Bu)<sub>3</sub>/B(C<sub>6</sub>F<sub>5</sub>)<sub>3</sub> to benzene and benzene-benzene RDFs using the ancillary SHARM routines within EPSR. These are shown in **Fig. 13-SI**. The closest contact correlation in the model is between benzene solvents and B(C<sub>6</sub>F<sub>5</sub>)<sub>3</sub> with a first peak at 4 Å followed by a broader less defined correlation with a maximum at 9 Å.

**Table 1-SI** Lennard-Jones potentials and Coulombic charges for PG and water used as the reference potential in the EPSR simulation.

Atom	$\epsilon / \text{kJ mol}^{-1}$	$\sigma / \text{\AA}$	$q_e$
PB	0.800	3.20	-0.2735
CB1	0.800	3.70	-0.2293
CB2	0.800	3.70	0.4033
HB1	0.000	0.00	-0.7800
BA1	0.800	3.20	0.2643
CA1	0.800	3.70	-0.1547
CA2	0.800	3.70	0.15543
FA1	0.800	3.20	-0.14211
C1	0.800	3.70	-0.59450
H1	0.000	0.00	0.59420

**Table 2-SI** Distance and angular restraints incorporated in initial *mol* input files for the EPSR model.

B(C <sub>6</sub> F <sub>5</sub> ) <sub>3</sub>	All angles defined as 120° with unrestricted rotation about B-C bonds	
BA1-CA1	1.562 Å	
CA1-CA2	1.436 Å	
CA2-CA2	1.436 Å	
CA2-FA1	1.320 Å	
Benzene	All angles defined at 120° with 0/180° dihedrals to fix planarity of ring	
C1-C1	1.405 Å	
C1-H1	1.089 Å	
( <sup>t</sup> Bu) <sub>3</sub> P	With unrestricted rotation around the P-C and C-C bonds	
PB-CB1	1.838 Å	CB1-PB-CB1 116.4°
CB1-CB2	1.550 Å	PB-CB1-CA1 110.6°
CB2-HB1	1.109 Å	CB1-CB2-HB1 108°
		HB1-CB2-HB1 106°

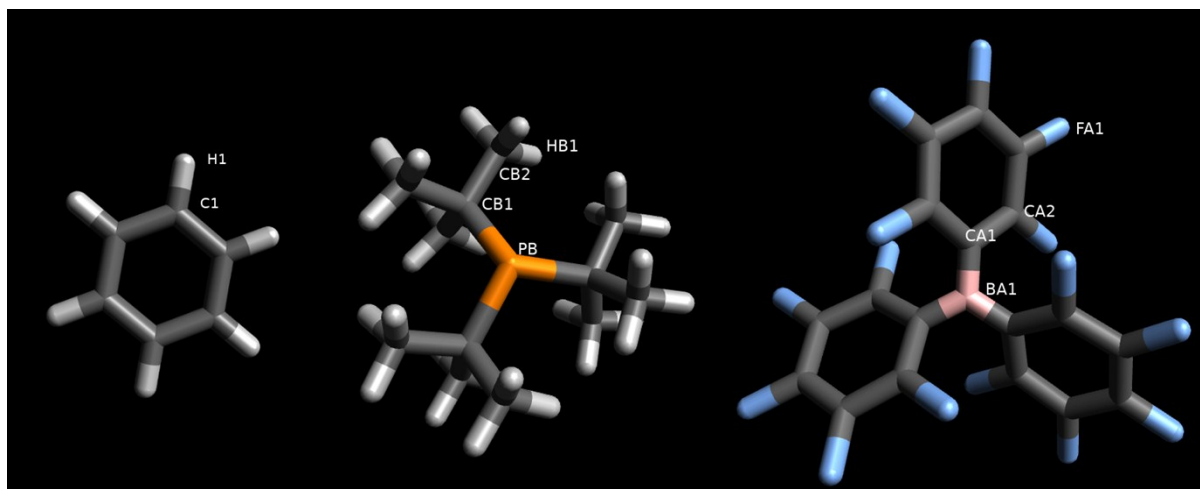


**Fig. 11-SI** Atom labels used to define for each unique atomic position in the molecular skeletons of the molecular components in the mixtures (benzene, P(<sup>t</sup>Bu)<sub>3</sub> and B(C<sub>6</sub>F<sub>5</sub>)<sub>3</sub>) for EPSR models.

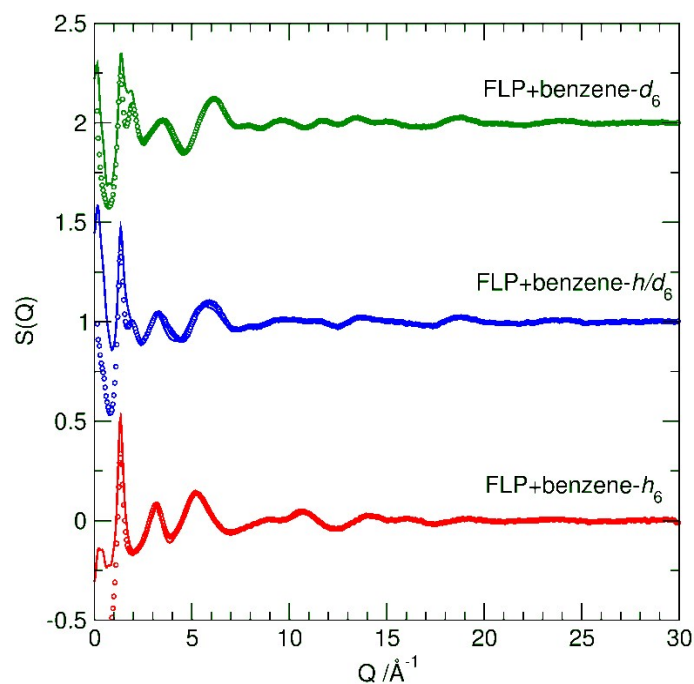


**Fig. 12-SI** Experimental (data points) and EPSR fitted (lines)  $S(Q)$  scattering for the three mixtures of  $t\text{Bu}_3\text{P}+\text{B}(\text{C}_6\text{F}_5)_3$  (1:1:70 ratio) in hydrogenous (red) deuterated (green) and 1:1 H/D mixed (blue) benzene.

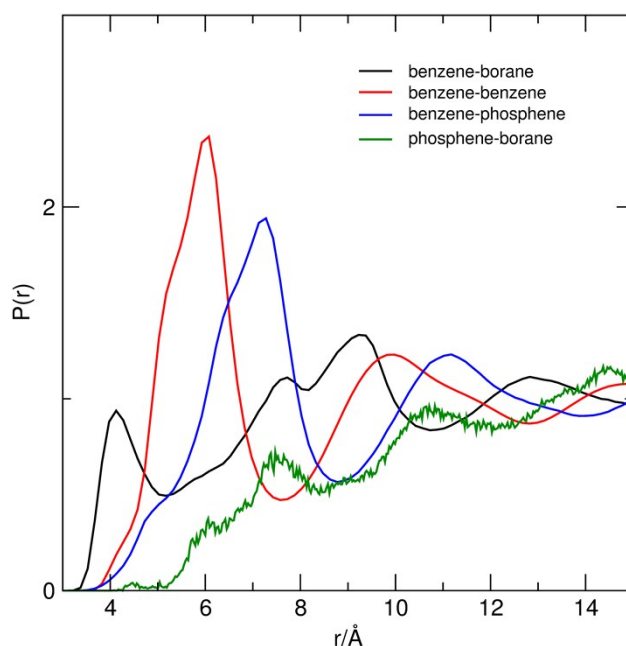


**Fig. 13-SI** Comparison of the small  $\text{P}(t\text{Bu})_3 \cdots \text{B}(\text{C}_6\text{F}_5)_3$  correlation in the EPSR model of the experimental data with the larger radial distribution functions (RDFs) between  $\text{B}(\text{C}_6\text{F}_5)_3$  and benzene (black),  $\text{P}(t\text{Bu})_3$  and benzene (blue) and the benzene-benzene self-correlation (red).

<sup>1</sup> G. C. Welch and D. W. Stephan, *J. Am. Chem. Soc.*, 2007, **129**, 1880.

<sup>2</sup> L. Rocchigiani, G. Ciancaleoni, C. Zuccaccia and A. Macchioni, *J. Am. Chem. Soc.*, 2014, **136**, 112

<sup>3</sup> A. K. Soper, *RAL Technical Report No. RAL-TR-201*, 2011

<sup>4</sup> A. K. Soper, *Chem. Phys.*, 1996, 202, 295; A. K. Soper, *Mol. Phys.*, 2001, **99**, 1503